

# **Electronic Supporting Information for Enhanced Stability and Activity for Water Oxidation in Alkaline Media with Bismuth Vanadate Photoelectrodes Modified with a Cobalt Oxide Catalytic Layer Produced by Atomic Layer Deposition**

Michael F. Lichterman<sup>1,2</sup>, Matthew R. Shaner<sup>1,2</sup>, Sheila G. Handler<sup>1,2</sup>, Bruce S. Brunschwig<sup>1,3</sup>, Harry B. Gray<sup>2,3\*</sup>, Nathan S. Lewis<sup>1,2,3,4\*</sup>, Joshua M. Spurgeon<sup>1,2\*</sup>

<sup>1</sup> Joint Center for Artificial Photosynthesis, California Institute of Technology, Pasadena, CA, 91125, USA

<sup>2</sup> Division of Chemistry and Chemical Engineering, California Institute of Technology, Pasadena, CA, 91125, USA

<sup>3</sup> Beckman Institute, California Institute of Technology, Pasadena, CA, 91125, USA

<sup>4</sup> Kavli Nanoscience Institute, California Institute of Technology, Pasadena, CA, 91125, USA

## Experimental

### Preparation of Electrodes

n-BiVO<sub>4</sub> electrodes were produced using a slight modification of published spin-coating procedures<sup>2</sup>. A stoichiometric solution of Bi(NO<sub>3</sub>)<sub>3</sub>•5H<sub>2</sub>O (Sigma Aldrich, 99.99%) and VO(acac)<sub>2</sub> (Sigma Aldrich, 98%) was prepared by making a solution of 398 mg of VO(acac)<sub>2</sub> in 50 mL 2,4-pentanedione (Acros, >99%) and a solution of 728 mg of Bi(NO<sub>3</sub>)<sub>3</sub>•5H<sub>2</sub>O in 7.5 mL 2,4-pentanedione. These solutions were then combined and mixed thoroughly. The resulting solution was spin-cast onto a slide of TEC-15 FTO glass (Hartford Glass) by masking the top 0.5 cm of glass using Scotch tape, coating the exposed area, and spinning twice at 1000 rpm for 6 s each time, per coating cycle, on a Laurell Technologies spin-coater with the acceleration set to 150. After each coating cycle, the tape was removed, and the glass was placed on a quartz holder and heated in an oven at 500 °C for 10 min. Nine deposition cycles were used to make BiVO<sub>4</sub> photoanodes; after the last coating cycle, the slide was sintered at 500 °C for 2 h. Figure S1 shows four FTO slides on a quartz plate after sintering, with a penny for size comparison. The slides were scored and broken into 1- × 2.5-cm pieces.

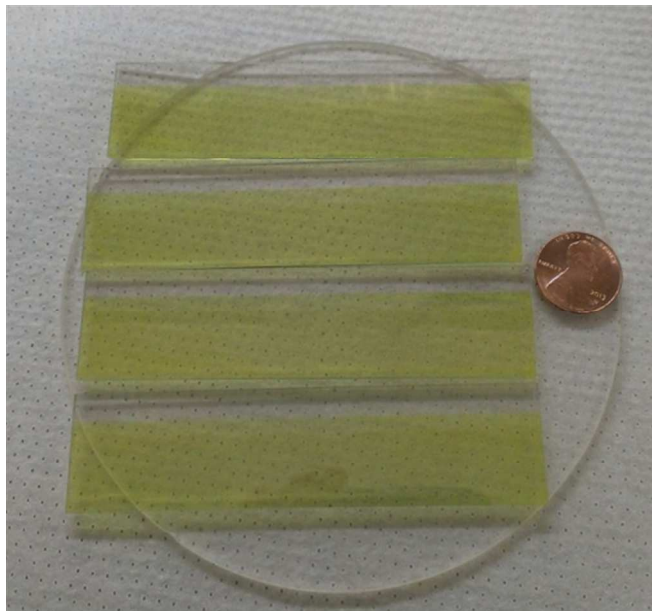


**Figure S1:** Multiple FTO slides being prepared with n-BiVO<sub>4</sub> simultaneously.

with the following purge with N<sub>2</sub>(g) at 20 cm<sup>3</sup> min<sup>-1</sup> for 15 s before an ozone pulse for 2 s and another purge for 15 s, to complete a full ALD cycle.

Cobalt oxide was deposited on n-BiVO<sub>4</sub>-coated slides following a published procedure<sup>3</sup>. Cobaltocene (Strem, >98%) was loaded into a canister in a glove box, and the canister was sealed using a gasket connection to a steel bellows valve. The canister was removed from the glove box and loaded onto the ALD instrument (Cambridge Nanotechnology) using another gasket fitting, and was heated by a heating sleeve. Ozone was created by a Del Ozone LG-7 Corona Discharge ozone generator. The cobaltocene was heated to 80 °C and the substrate was maintained at 150 °C. The cobaltocene precursor was pulsed for 5 s,

The finished CoO<sub>x</sub>/n-BiVO<sub>4</sub>/FTO slides were made into electrodes ~1 cm wide by 1 cm in length. Electrical contact between the electrode and a wire was made using Ag paint, and the entire contact and any exposed FTO glass was covered with non-conductive epoxy. The epoxy was used to mask the exposed area of electrode to 1 cm<sup>2</sup>. The wire was encased in a glass tube and the end of the tube epoxied to the contacting assembly to allow for O<sub>2</sub>-production experiments.

## Characterization of Electrodes

Spectral response characterization measurements were performed using a 300 W Xe lamp and monochromator (Newport Oriel Instruments) and lock-in amplifiers (Stanford Research Instruments). XPS measurements were performed with an M-probe spectrometer (VG-Surface Science Instruments, Pleasanton, CA) at a nominal base pressure of ca.  $1 \times 10^{-8}$  Torr. The excitation for XPS was provided by monochromatic Al K $\alpha$  X-rays (1486.6 eV) incident at 35° with respect to the surface plane and with an elliptical focused-beam size of 250  $\times$  1000  $\mu$ m. The emitted photoelectrons were collected into a hemispherical energy analyzer at a takeoff angle identical to the angle of incidence, with a retarding (pass) energy of 154.97 eV. XPS data were fitted using Hawk 7 software (V7.03.04; Service Physics, Bend, OR) and were referenced to the adventitious carbon peak at 284.6 eV. Photoelectrochemical and impedance experiments were performed using a Bio-Logic SP-200 potentiostat.

*J-E* measurements were performed using a 3- or 4-neck 50-mL round-bottom flask that had been modified with a planar quartz window. The wattage of the Xe lamp (Newport) used for illumination could be varied to produce the desired incident illumination power. The light intensity was adjusted to produce the same short-circuit current density as produced by 100 mW cm<sup>-2</sup> of AM1.5G sunlight on a secondary standard Si photodiode. A three-electrode configuration was used with a SCE or a Ag/AgCl reference electrode (BAS Inc.) and a Pt gauze counter electrode located in a fritted compartment that contained the same pH 13 electrolyte as contained in the main cell compartment.

For O<sub>2</sub>(g) evolution experiments, a Neofix fluorescence probe was used in an airtight cell, along with a Ag/AgCl reference electrode. The Pt gauze counter electrode was positioned in a separate, fritted compartment. The cell volume was 51 mL, and the cell was purged with a stream of Ar(g) for ~1 h prior to data collection. The experiment was run for 30 min after a 10-min waiting period at open circuit.

UV-Vis spectroscopy was performed using a Shimadzu Solidspec-3700 spectrometer with an integrating sphere for diffuse/specular reflectance measurements. Atomic force microscopy (AFM) measurements were performed using a Bruker Dimension Icon.

## Further Results

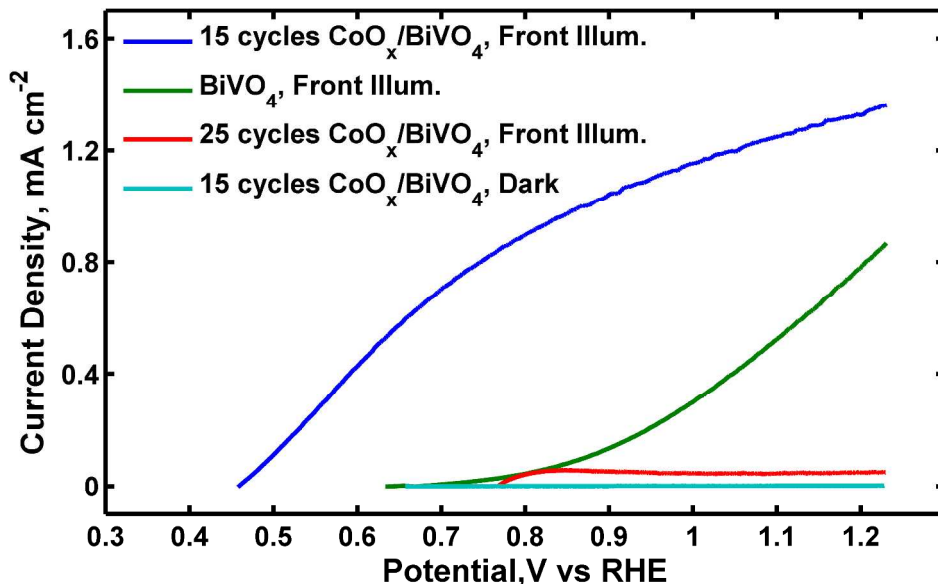


**Figure S2:** Linear Sweep Voltammograms of plain BiVO<sub>4</sub>, BiVO<sub>4</sub> with 15 ALD cycles of cobalt oxide, and BiVO<sub>4</sub> with 25 ALD cycles of cobalt oxide.

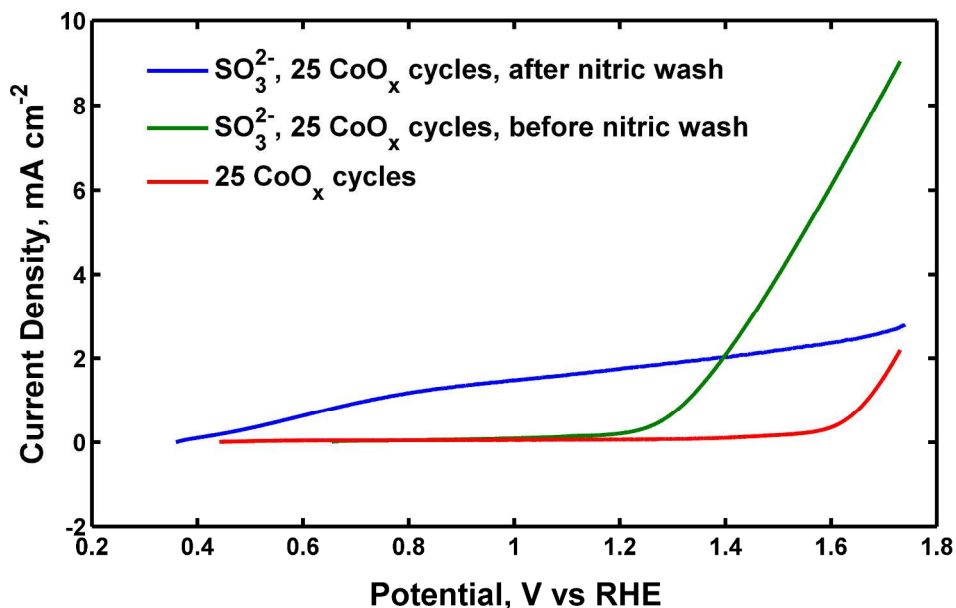


**Figure S3:** Linear Sweep Voltammograms under 1 sun illumination at pH 13 of 25 ALD cycles of CoO<sub>x</sub> on BiVO<sub>4</sub>, 25 ALD cycles of CoO<sub>x</sub> on BiVO<sub>4</sub> with sodium sulfite present as a sacrificial hole acceptor, and 25 ALD cycles of CoO<sub>x</sub> on BiVO<sub>4</sub> with sulfite present after the electrode has been briefly washed with 1.0 M nitric acid. The 1.0 M nitric acid wash produced an electrode that displayed effectively identical photoelectrochemical behavior to an electrode that had no CoO<sub>x</sub> present, or one with fewer cycles of CoO<sub>x</sub>.

## Spectral Response

Figure S4 shows the spectral response data for the  $\text{CoO}_x/\text{n-BiVO}_4$  and for the unmodified  $\text{n-BiVO}_4$  electrodes, as a function of the electrode potential vs RHE. As would be expected from the  $J-E$  data, more positive potentials produced larger anodic photocurrents, corresponding to a higher quantum efficiency as the electrode potential increased.

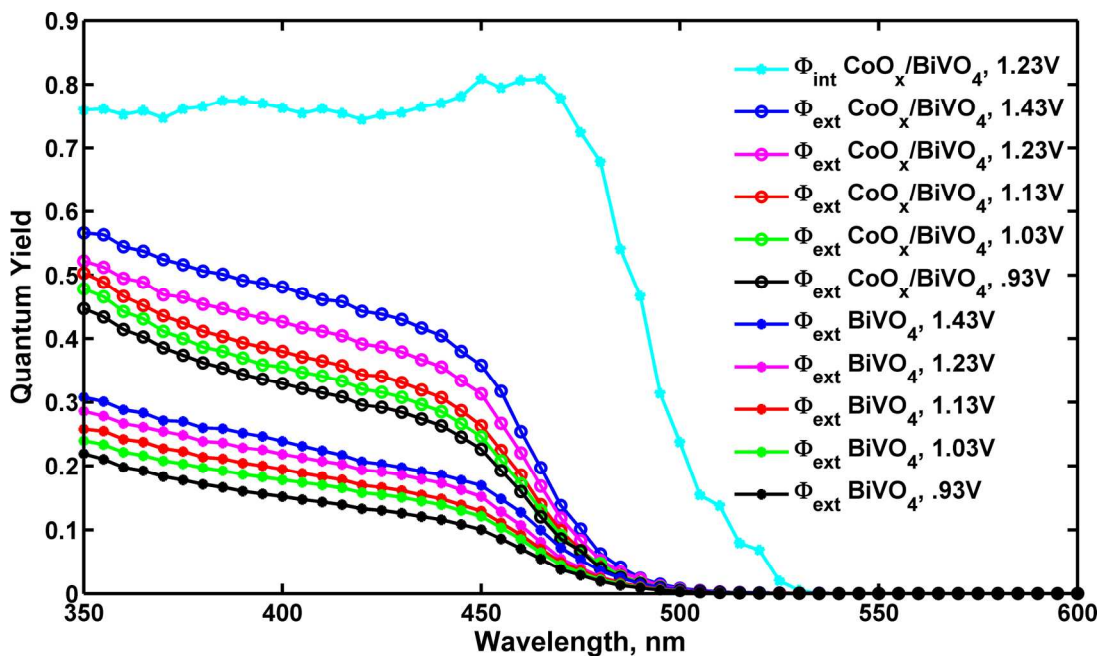


Figure S4: Quantum Yield measurements at multiple potentials vs. RHE

## Calculations for Spectral Response

A calibrated silicon photodiode with known spectral responsivity from Thor Labs was used to calibrate the apparatus. The electrode of interest (calibrated Si or  $(\text{CoO}_x)/\text{BiVO}_4$  electrode) was attached to a potentiostat, which relayed chopped current data to a lock-in-amplifier, from which data was collected as current and normalized by an internal photodiode. The collected photoresponse was divided by the maximum photoresponse expected at each wavelength as determined from the calibrated diode in order to determine the Incident Photon to Current Efficiency (External Quantum Yield). Absorbed Photon to Current Efficiency (Internal Quantum Yield) was found by simply dividing this number by the absorbance as described in the text.

Integrating the results for External Quantum Yield from the data at 1.23 V vs. RHE against the tabulated AM 1.5G spectral intensity from gave a predicted current density of  $2.03\text{mA cm}^{-2}$ , which indicates that the performance of this system may be slightly underestimated by analysis of the  $J$ - $E$  data described herein. The ASTM G-173, Global tilt, data were used as the source spectrum.

## XPS Spectra

Figure S5 shows the XPS spectra for Bi, V, O and Co for an electrode (a) after deposition of the cobalt oxide (and exposure to standard atmosphere), (b) after 10 cyclic voltammetric cycles and (c) after 30 min at 0.97 V vs. RHE under photoanodic operation at pH 13. The cobalt oxide signals indicated the presence of  $\text{Co}_3\text{O}_4$  in all scans, although the initial signals also demonstrated the formation of  $\text{Co}(\text{OH})_2$  or  $\text{CoO}$ , as indicated by presence of a strong satellite peak at 786 eV. Only the  $\text{Co } 2p^{3/2}$  peak is shown, because the  $\text{Co } 2p^{1/2}$  peak was very close in energy to the  $\text{Bi } 4p^{1/2}$  peak. On peaks where multiple constituent peaks are summed, the individual peaks are displayed in blue and the summed model is displayed in purple. For peak models made of only one constituent peak, the single constituent is shown in purple.

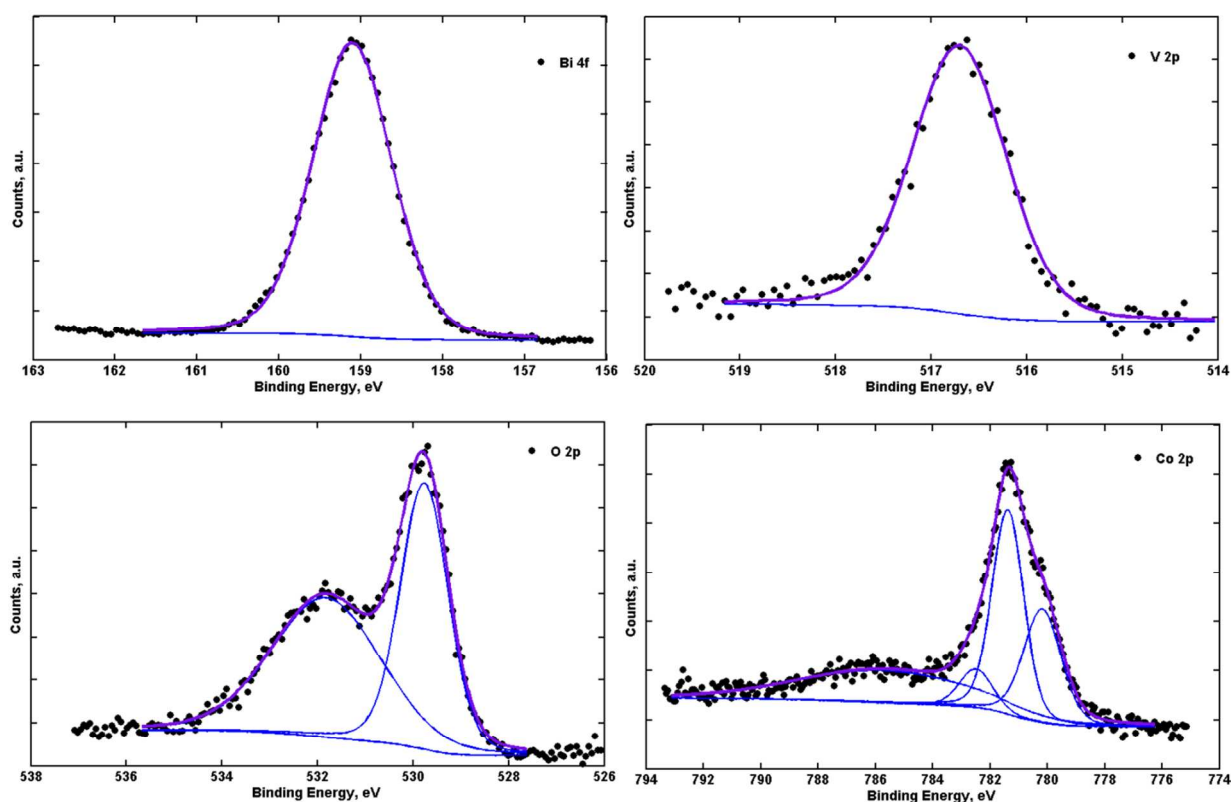
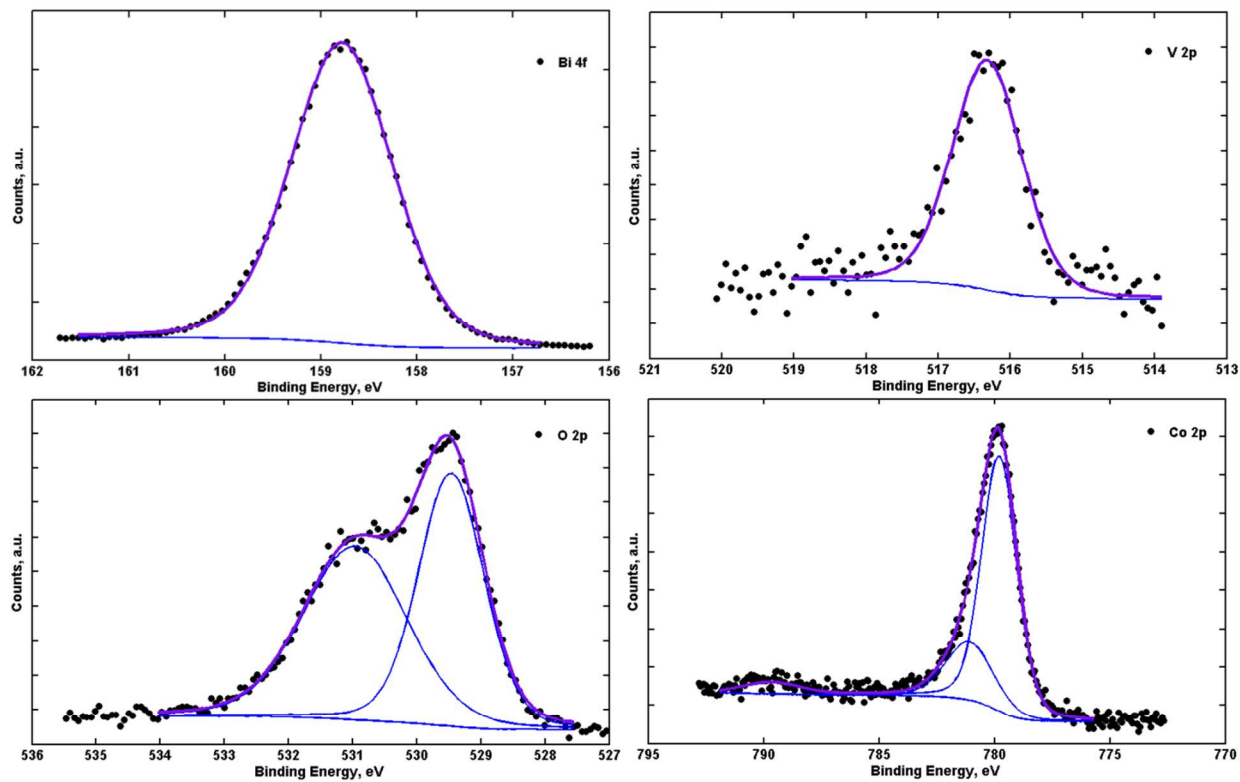
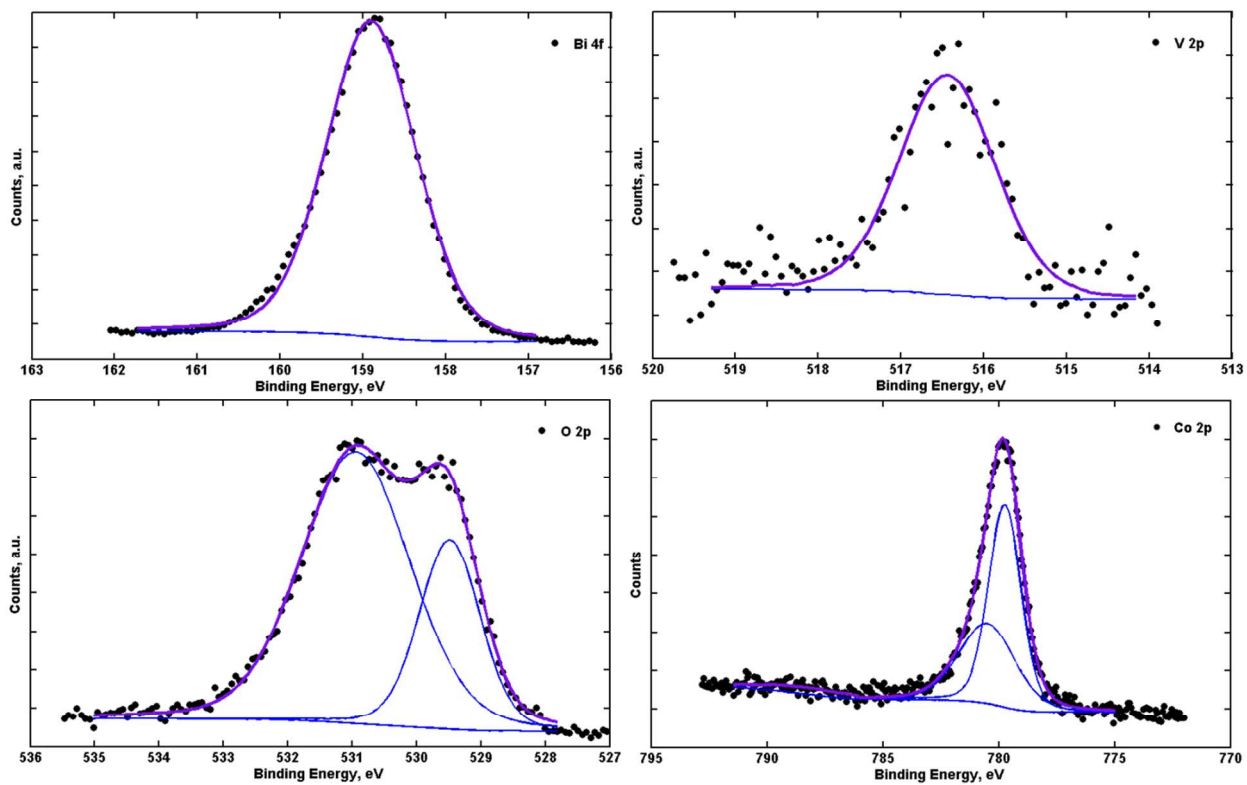


Figure S5a: XPS spectra taken after cobalt oxide deposition.



**Figure S5b:** XPS data after 10 cyclic voltammetric sweeps.





**Figure S5c:** XPS data after 30 min of photoanodic operation under illumination at 0.97 V vs. RHE in pH 13 KOH(aq).

Figure S6 contains data for 200 ALD cycles of  $\text{CoO}_x$  on FTO under a similar set of conditions: (a) after deposition, (b) after 10 cyclic voltammogram (CV) sweeps to  $1.5\text{mA cm}^{-2}$ , and (c) after 30 minutes of galvanostatic current flow at  $1.5\text{ mA cm}^{-2}$ .

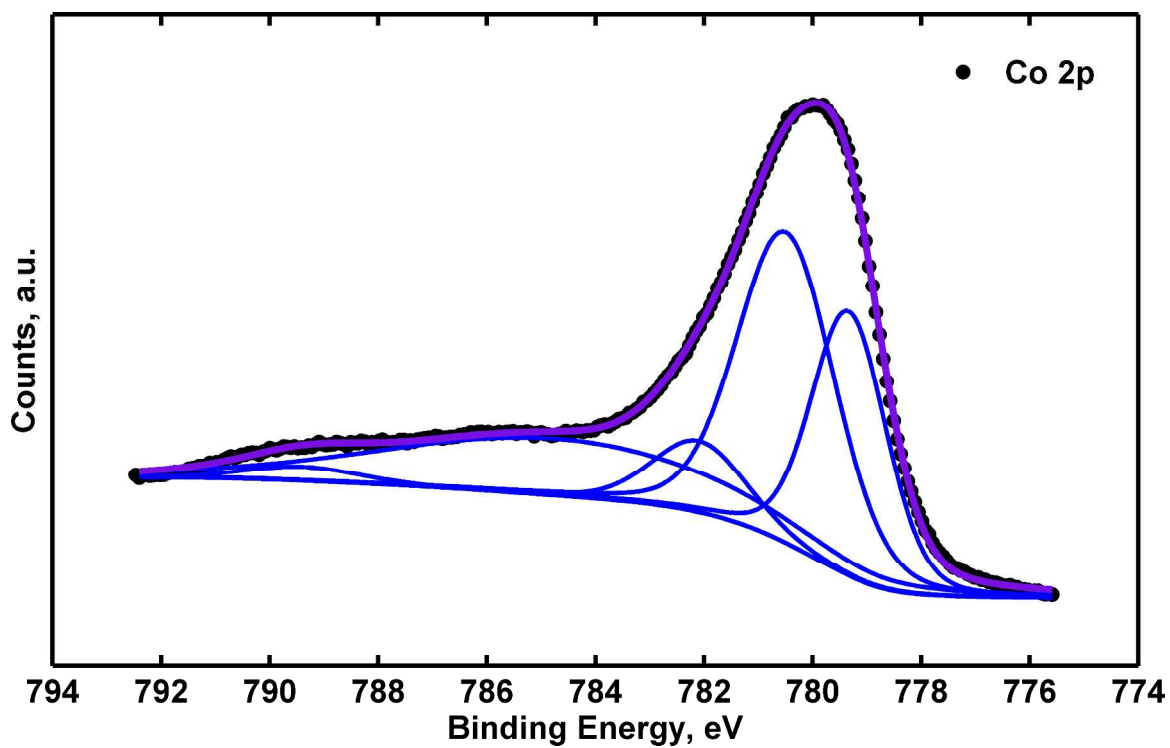


**Figure S6a:** XPS data for cobalt for 200 cycles of  $\text{CoO}_x$  deposited on FTO, directly after deposition.

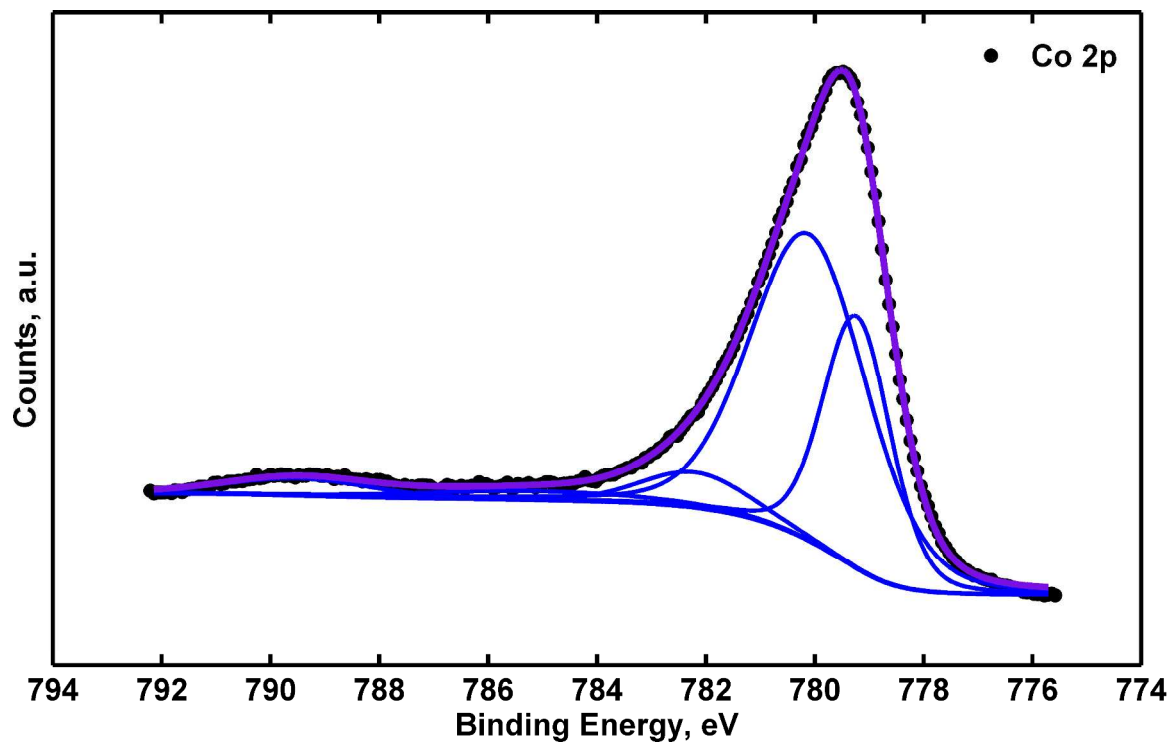


**Figure S6b:** XPS data for cobalt for 200 cycles of  $\text{CoO}_x$  after 10 CV sweeps.

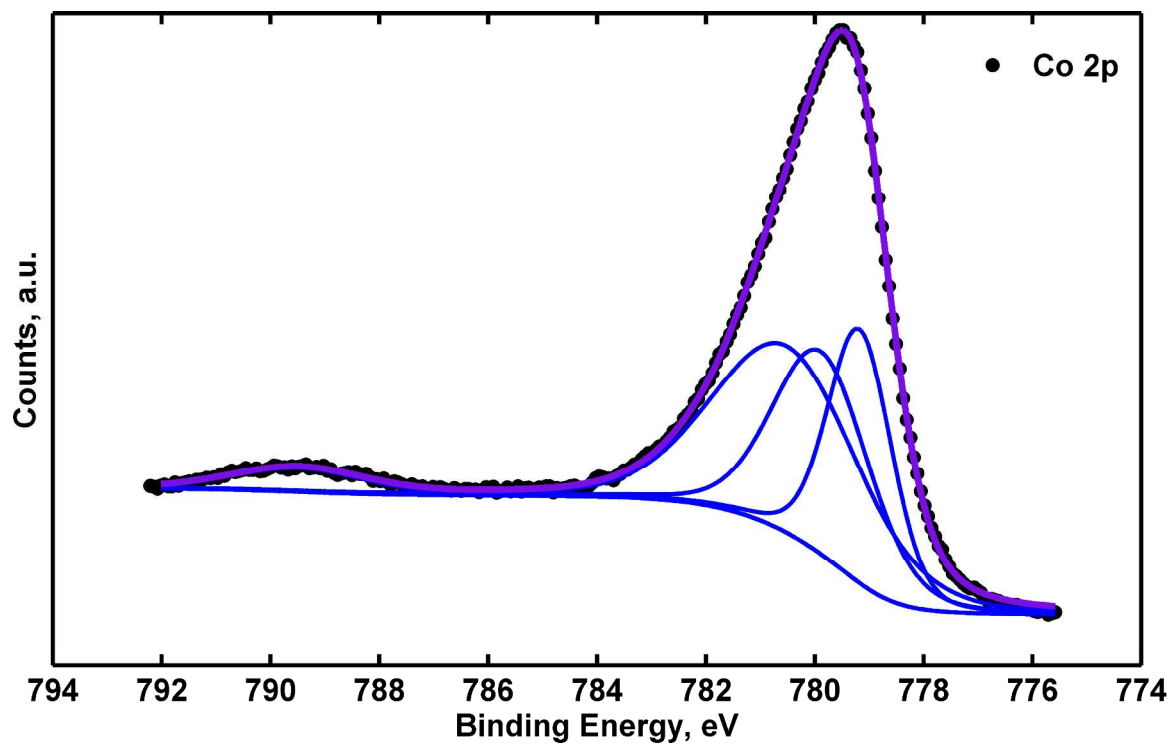


**Figure S6c:** XPS data for cobalt for 200 cycles of  $\text{CoO}_x$  after 30 minutes of OER catalysis.

While the small amount of CoO<sub>x</sub> on the active CoO<sub>x</sub>/BiVO<sub>4</sub> samples does not allow for a definitive assignment of the oxidation state of the cobalt, the thicker films formed from 200 ALD cycles allow for a concise determination of the form of cobalt oxide present. The large shoulder near 786 eV in the as-deposited sample clearly present in both the CoO<sub>x</sub>/BiVO<sub>4</sub> samples as well as the thick CoO<sub>x</sub> samples indicates that the cobalt oxide as-deposited contains a significant fraction of Co(II), likely as Co(OH)<sub>2</sub> or CoO, in addition to Co<sub>3</sub>O<sub>4</sub> or CoOOH which is indicated by the satellite near 790 eV.<sup>4</sup> However, even a brief amount of current flow leads to a quick change in the spectra for the cobalt, in which the satellite near 786 eV disappears almost entirely (Fig. S7b) and then entirely (Fig. S7c), leaving only the main peak at 780 eV and the satellite at 790 eV with no satellite at 786 eV. This strongly suggests the active form for water oxidation in pH 13 is CoOOH.<sup>4</sup>

## Thickness Determination

Overlayer thicknesses were modelled using the equation<sup>5</sup>

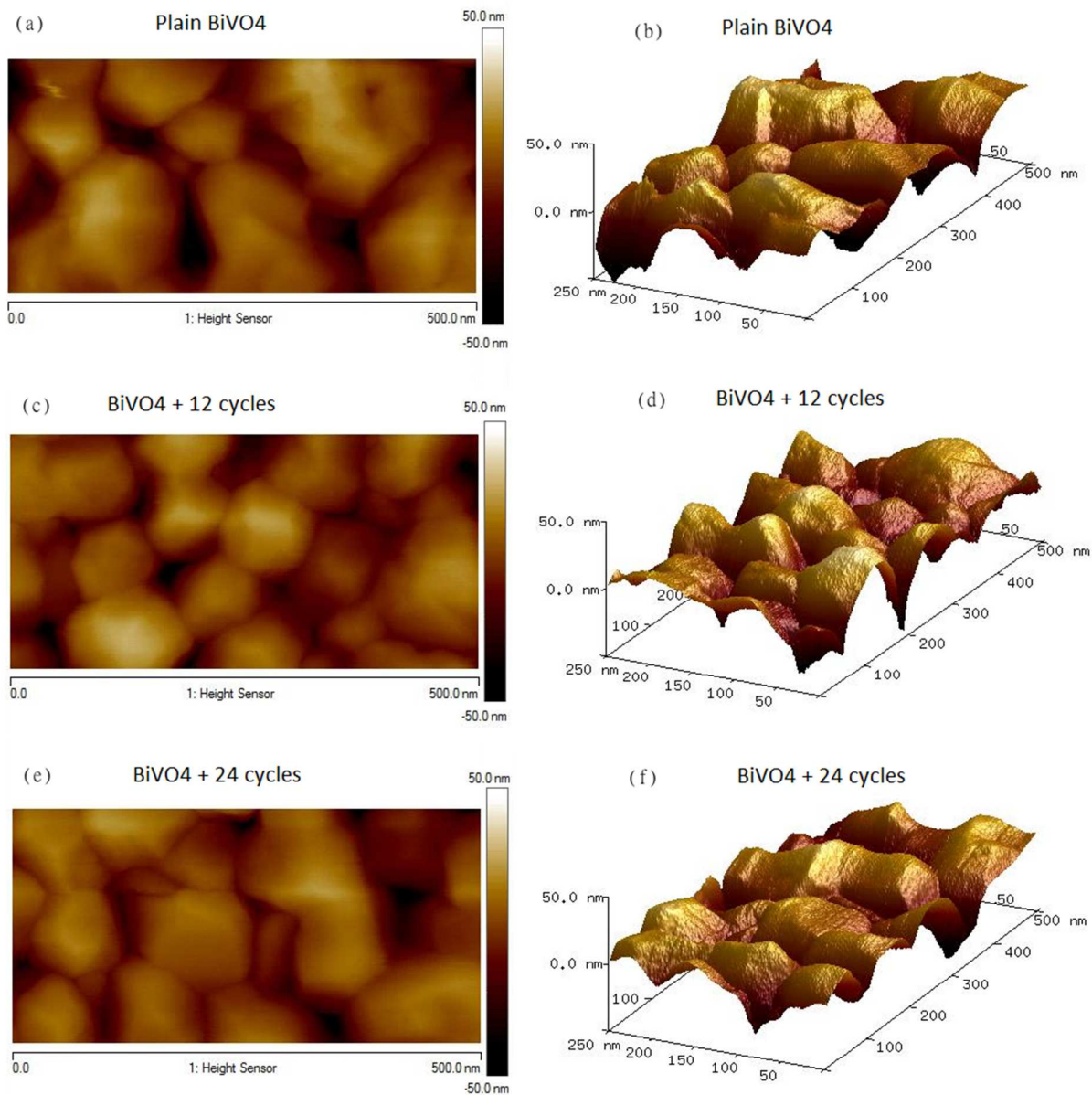
$$\left(\frac{I_{\text{Co}}}{I_{\text{Bi}}}\right)\left(\frac{\text{SF}_{\text{Bi}}}{\text{SF}_{\text{Co}}}\right)\left(\frac{\rho_{\text{Bi}}}{\rho_{\text{Co}}}\right) = \exp\left(\frac{d_{\text{ov}}}{\lambda_{\text{Bi}} \sin\theta}\right) - \exp\left[-\left(\frac{d_{\text{ov}}}{\lambda_{\text{Co}} \sin\theta}\right) + \left(\frac{d_{\text{ov}}}{\lambda_{\text{Bi}} \sin\theta}\right)\right]$$

where  $I_{\text{Co}}$  and  $I_{\text{Bi}}$  are the respective normalized intensities, given by the peak area divided by number of scans, of the Co 2p<sup>3/2</sup> and Bi 4f<sup>7/2</sup> peaks in the XPS spectra.  $\text{SF}_{\text{Bi}}$  and  $\text{SF}_{\text{Co}}$  are the sensitivity factors for Co 2p<sup>3/2</sup> and Bi 4f<sup>7/2</sup> peaks, respectively;  $\rho_{\text{Bi}}$  and  $\rho_{\text{Co}}$  the corresponding atomic densities.  $\lambda_{\text{Bi}}$  and  $\lambda_{\text{Co}}$  are the attenuation depths for photoelectrons at either 160 eV (for  $\lambda_{\text{Bi}}$ ) or 780 eV (for  $\lambda_{\text{Co}}$ ), and were given by an online database based on published work.<sup>6</sup>  $d_{\text{ov}}$  is the thickness of the cobalt oxide overlayer, and  $\theta$  is 35°. The database provided values of 25.8 nm for  $\lambda_{\text{Bi}}$  and 69.2 nm for  $\lambda_{\text{Co}}$ . With the above data,  $d_{\text{ov}}$  was calculated as 0.9 nm for 20 ALD cycles, which is a reasonable result, since the ALD procedure followed here has been previously determined to produce a growth rate of 0.05 nm per cycle.<sup>3</sup>

## Atomic Force Microscopy

Atomic Force Microscopy (AFM) was used to investigate the surface before and after deposition of the catalyst layer.

**Figure S7** (a-f) displays representative 2-D and 3-D images of (a,b) the unmodified n-BiVO<sub>4</sub> electrode, (c,d) n-BiVO<sub>4</sub> with 12 ALD cycles of CoO<sub>x</sub>, and (e,f) n-BiVO<sub>4</sub> with 24 ALD cycles of CoO<sub>x</sub>.



## Further *J-E* Characterization

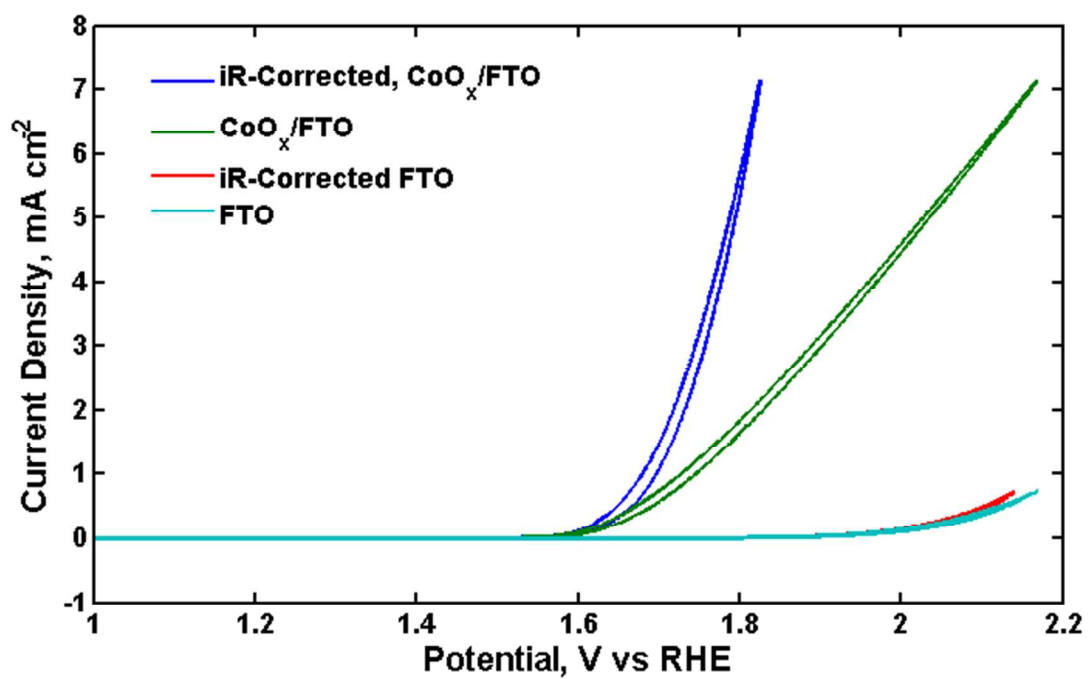


**Figure S8:** CoO<sub>x</sub>/FTO and plain FTO activity for OER, un-corrected and iR-corrected, at pH 13.

## Calculations for Oxygen Measurement and Faradaic Efficiency

The data were collected and modeled using a Matlab script. The data from the fluorescence probe were converted into micrograms of O<sub>2</sub> by first correcting for any O<sub>2</sub> leaks during the first 10 min of the experiment, followed by multiplying the reported percentage of oxygen by the number of micrograms of O<sub>2</sub> dissolved in water under these conditions (7700 μg/L) as well as by the cell volume (51.5 mL), and dividing by the density of O<sub>2</sub> in standard air, which was in the form reported by the probe(20.9). This process produced the mass of O<sub>2</sub> in micrograms at each time point. To calculate the charge vs time data from the potentiostat, the amount of charge passed (in mAh) was multiplied by 3.6 to convert the data into coulombs. This value was then multiplied by 83 to convert the value into micrograms of O<sub>2</sub>, since this constant equals the conversion factor of 1 coulomb of electrons into 1 microgram of O<sub>2</sub>.



## References

1. Seabold, J. A.; Choi, K.-S. Efficient and Stable Photo-Oxidation of Water by a Bismuth Vanadate Photoanode Coupled with an Iron Oxyhydroxide Oxygen Evolution Catalyst. *J. Am. Chem. Soc.* **2012**, *134*, 2186-2192.
2. Jeon, T. H.; Choi, W.; Park, H. Cobalt-Phosphate Complexes Catalyze the Photoelectrochemical Water Oxidation of BiVO<sub>4</sub> Electrodes. *Phys. Chem. Chem. Phys.* **2011**, *13*, 21392-21401.
3. Donders, M. E.; Knoops, H.; Van de Sanden, M. C.; Kessels, W. M.; Notten, P. Remote Plasma Atomic Layer Deposition of Co<sub>3</sub>O<sub>4</sub> Thin Films. *ECS Trans.* **2009**, *25*, 39-47.
4. Biesinger, M. C.; Payne, B. P.; Grosvenor, A. P.; Lau, L. W. M.; Gerson, A. R.; Smart, R. S. C. Resolving surface chemical states in XPS analysis of first row transition metals, oxides and hydroxides: Cr, Mn, Fe, Co and Ni. *Appl. Surf. Sci.* **2011**, *257*, 2717-2730.
5. Haber, J. A.; Lewis, N. S. Infrared and X-ray Photoelectron Spectroscopic Studies of the Reactions of Hydrogen-Terminated Crystalline Si(111) and Si(100) Surfaces with Br<sub>2</sub>, I<sub>2</sub>, and Ferrocenium in Alcohol Solvents. *J. Phys. Chem. B* **2002**, *106*, 3639-3656.
6. Henke, B. L.; Gullikson, E. M.; Davis, J. C. X-Ray Interactions: Photoabsorption, Scattering, Transmission, and Reflection at E = 50-30,000 eV, Z = 1-92. *Atomic Data and Nuclear Data Tables* **1993**, *54*, 181-342.